

Thermal and electrical transport in single crystalline MgB₂

A.V. Sologubenko, J. Jun, S. M. Kazakov, J. Karpinski, H.R. Ott
 Laboratorium für Festkörperphysik, ETH Hönggerberg, CH-8093 Zürich, Switzerland
 (Dated: October 30, 2018)

We present the results of measurements of the thermal and electrical conductivity in the basal plane of single-crystalline MgB₂ between 2 and 300 K. The analysis of the temperature dependence of the thermal conductivity gives supporting evidence for two different gaps on different sheets of the Fermi surface in the superconducting state. The zero-temperature values of the two gaps are $\Delta_1(0) = 5.3 \pm 0.5$ meV and $\Delta_2(0) = 1.65 \pm 0.2$ meV.

PACS numbers: 74.25.Fy, 74.70.-b, 74.25.Kc, 72.15.Eb,

The recent discovery of superconductivity in MgB₂ below an unexpectedly high critical temperature T_c of the order of 40 K initiated intensive studies of its physical properties [1]. Numerous results indicate that the superconducting state of MgB₂ is well described by the original BCS theory. Most experiments are compatible with a nodeless superconducting order parameter and imply that the electron-phonon interaction is responsible for the pairing of the electrons [2]. However, various types of experiments (see Ref. [3] and references therein), mainly using powder or polycrystalline samples, have given evidence for two gaps in the quasiparticle excitation spectrum of this superconductor. Qualitative and especially quantitative experimental checks of this intriguing situation on single crystalline material seem in order.

Below we present results of measurements of the thermal conductivity κ and the electrical resistivity ρ parallel to the basal ab -plane of the hexagonal crystal lattice of MgB₂ as a function of temperature T between 2 and 300 K. We demonstrate that our low-temperature results cannot be explained in terms of a single-gap function below the critical temperature, but are well approximated by assuming two different energy gaps in the superconducting state.

The investigated single crystal with dimensions of $0.5 \times 0.17 \times 0.035$ mm³ was grown with a high-pressure cubic anvil technique as described elsewhere [4]. The resistivity was measured by employing a 4-contact configuration in the ab -plane. For the thermal conductivity measurements, the standard method with a constant uniaxial heat flow was used. The same contacts were used for measuring the voltage and the temperature difference, respectively. Additional measurements of $\rho(T)$ and $\kappa(T)$ in constant magnetic fields H , oriented along the hexagonal c -axis, were made as well.

The electrical resistivity $\rho(T)$ in zero magnetic field is presented in Fig. 1. The narrow ($\Delta T_c = 0.1$ K) superconducting transition occurs at $T_c = 38.1$ K. In the temperature region between T_c and 130 K, $\rho(T)$ may be well approximated by $\rho = \rho_0 + A'T^3$, where ρ_0 and A' are constants. At temperatures below 50 K, $\rho \approx \rho_0 = 2.0$ $\mu\Omega$ cm. A cubic $\rho(T)$ dependence has often been observed in transition metals and is associated with interband electron-

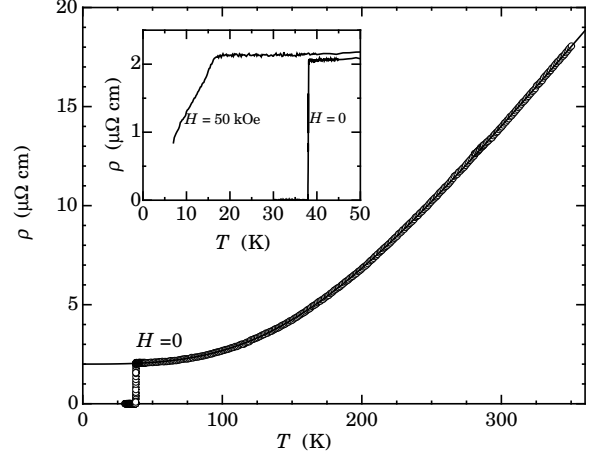


FIG. 1: In-plane electrical resistivity $\rho(T)$ of hexagonal MgB₂. The inset emphasizes the low temperature part for $H = 0$ and 50 kOe along the c -axis.

phonon scattering[5, 6]. The corresponding equation

$$\rho(T) = \rho_0 + AT^3 J_3(\Theta_R/T), \quad (1)$$

where $J_n(z) = \int_0^z x^n e^x (1 - e^x)^{-2} dx$, fits our data perfectly. This is demonstrated by the solid line in Fig. 1. A similar fit to data from polycrystalline material is presented in Ref. [7]. The fit parameters A and Θ_R characterize the strength of electron-phonon interaction and the cut-off frequency ω_{\max} of the phonon spectrum, respectively. The fit value of $\Theta_R = 1226$ K is in excellent agreement with the value of $\hbar\omega_{\max} = 105$ meV measured in inelastic neutron scattering experiments [8, 9]. The magnitude of Θ_R is considerably higher than the Debye temperature $\Theta_D \sim 700 - 900$ K, extracted from low-temperature specific heat measurements [10, 11, 12]. This discrepancy is not unexpected because electrical resistivity and specific heat involve different averages of the lattice frequencies [13].

The inset of Fig. 1 emphasizes $\rho(T)$ close to the superconducting transitions in fields of $H = 0$ and $H = 50$ kOe. For $H = 50$ kOe, the critical temperature, marked by the onset of the deviation from the constant

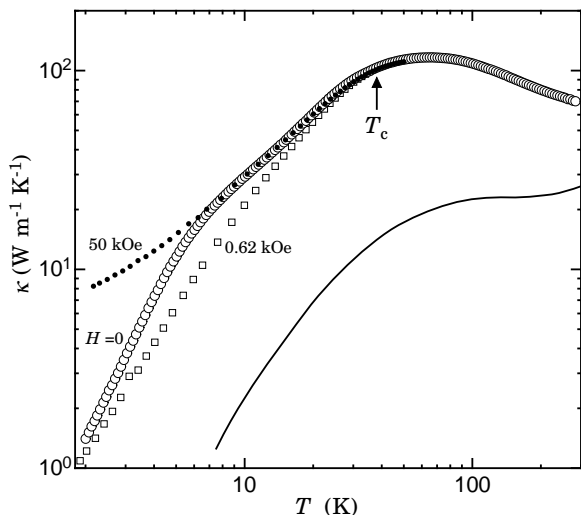


FIG. 2: Thermal conductivity vs temperature in the *ab*-plane of MgB₂ in zero magnetic field and for $H = 0.62$ kOe and 50 kOe parallel to the *c*-axis. The solid line represents the typical zero-field behavior of $\kappa(T)$ measured on polycrystalline samples (data from Ref. [15]).

resistivity in the normal state, is shifted to $T_c = 17$ K.

The thermal conductivity data $\kappa(T)$ in zero magnetic field and for $H = 0.62$ and 50 kOe are presented in Fig. 2. The zero-field $\kappa(T)$ values are about an order of magnitude higher than previously reported for polycrystalline samples [7, 14, 15, 16]. Also the temperature dependence of κ is quite different from those earlier data. Instead of a monotonous increase with temperature we note a distinct maximum of $\kappa(T)$ at $T \sim 65$ K. No anomaly in $\kappa(T)$ provides evidence for the transition at T_c . A pronounced slope change in $\kappa(T)$ is observed around $T \sim 6$ K, however.

The thermal conduction of a superconductor is usually provided by electrons (κ_e) and phonons (κ_{ph}), such that

$$\kappa = \kappa_e + \kappa_{ph}. \quad (2)$$

A separate identification of these two terms at arbitrary temperature is not straightforward. In the normal state, a convenient and often used way to estimate κ_e is to employ the Wiedemann-Franz law, which relates the electrical resistivity and the electronic contribution to the thermal conductivity via

$$\kappa_e(T) = L_0 T / \rho(T), \quad (3)$$

where $L_0 = 2.45 \times 10^{-8}$ W Ω K⁻² is the Lorenz number. The validity of this law requires an elastic scattering of electrons and it is well established that Eq. (3) is applicable if the scattering of electrons by defects dominates. This is usually true at low temperatures, where $\rho(T) \approx \rho_0$. At higher temperatures but below Θ_D ,

Eq. (3) is usually invalid. In our case, the regime of applicability of Eq. (3) is limited to temperatures below about 50 K (see Fig. 1). At temperatures $T_c \geq T \geq 50$ K, $\kappa_e(T)$ provides about half of the total thermal conductivity.

Upon decreasing the temperature below T_c , the reduction of the number of unpaired electrons leads to a decrease of κ_e and an increasing κ_{ph} . The overall behavior of $\kappa(T)$ in the superconducting state depends on the relative magnitudes of κ_e and κ_{ph} and also on the strength of electron-phonon interaction. Using existing theoretical models, $\kappa(T)$ data may provide valuable information about the superconducting gap function. In the following, we restrict our analysis of $\kappa(T)$ to temperatures below 50 K, where the separation of κ_e and κ_{ph} can reliably be accomplished.

The electronic contribution to $\kappa(T)$ in the superconducting state has been calculated by Bardeen, Rickayzen, and Tewordt [17]. In their model

$$\kappa_e = \kappa_{e,n} f(y), \quad (4)$$

where

$$f(y) = \frac{2F_1(-y) + 2y \ln(1 + e^{-y}) + \frac{y^2}{1+e^y}}{2F_1(0)}, \quad (T < T_c)$$

$$\text{and} \quad (5)$$

$$f(y) = 1, \quad (T \geq T_c),$$

as well as $F_n(-y) = \int_0^\infty z^n (1 + e^{z+y})^{-1} dz$, $y = \Delta(T)/k_B T$, and $\Delta(T)$ representing the energy gap. Here $\kappa_{e,n}$ is the normal-state electronic thermal conductivity and in our analysis $\kappa_{e,n} = L_0 T / \rho_0$.

The phonon thermal conductivity was analyzed in terms of the Debye-type relaxation rate approximation. The corresponding equation is [18]

$$\kappa_{ph} = \frac{k_B}{2\pi^2 v} \left(\frac{k_B}{\hbar} \right)^3 T^3 \int_0^{\Theta_D/T} \frac{x^4 e^x}{(e^x - 1)^2} \tau(\omega, T) dx, \quad (6)$$

where ω is the frequency of a phonon, $\tau(\omega, T)$ is the corresponding relaxation time, $v = \Theta_D (k_B/\hbar) (6\pi^2 n)^{-1/3}$ is the average sound velocity, n is the number density of atoms, and $x = \hbar\omega/k_B T$. For our analysis, we use $\Theta_D = 750$ K, as deduced from specific heat measurements [10, 11]. The total phonon relaxation rate

$$\tau^{-1} = L/v + B\omega^4 + CT\omega^2 \exp(-\Theta_D/bT) + D\omega + E\omega g(x, y) \quad (7)$$

can be represented as a sum of terms corresponding to independent scattering mechanisms. The individual terms, dominating in different temperature intervals, introduce phonon scattering by sample boundaries, point defects, phonons, dislocations, and electrons, respectively. The constants L , B , C , b , D , and E are a measure for the intensity of corresponding phonon relaxation processes.

The function $g(x, y)$ is given in Ref. [17]; we do not reproduce its rather complex form here.

For $H = 50$ kOe the phonon contribution $\kappa_{\text{ph}}(T)$ in the normal state (above 17 K), extracted from $\kappa(T)$ and $\rho(T)$ using Eqs. (2) and (3), is identical to $\kappa_{\text{ph}}(T)$ calculated for $H = 0$ above T_c . We thus conclude that magnetic field effects on κ_{ph} are negligible. Based on the assumption that phonon scattering by both defects and phonons is the same in the normal and in the superconducting state, we estimate the temperature region where the number of unpaired electrons is too small to produce significant contributions to both phonon scattering and heat transport. Taking into account the lowest previously claimed value of $\Delta(0) = 1.7$ meV [19], the electronic quasiparticles are effectively excluded from heat transport below 4 K.

The following analysis procedure is based on the assumptions discussed above. In a first step, the values of the parameters L , B , C , b , D , and E , related to the processes of phonon relaxation in the normal state, were obtained by fitting the $\kappa_{\text{ph}}(T)$ data in $H = 50$ kOe above 17 K (for this region $g(x, y) = 1$) to Eqs. (6) and (7) as well as $\kappa(T)$ below 4 K where $g(x, y) = 0$ and $\kappa_e = 0$. These fits are shown in the inset of Fig. 3. The values of the parameters, common for both fits, are $L = 2.6 \times 10^{-4}$ m, $B = 1.07 \times 10^{-3}$ s³, $C = 3.0 \times 10^{-18}$ s K⁻¹, $b = 6.2$, $D = 2.1 \times 10^{-5}$, and $E = 7.5 \times 10^{-5}$. We refrain from a detailed discussion of the parameters related to defect, boundary, and phonon-phonon scattering, and in the subsequent analysis we consider them as serving as a background. Our primary interest is the electron-phonon interaction represented by the parameter E . The value of E obviously fixes the shift between the two broken lines in the inset of Fig. 3. We note that the value of E is quite robust with respect to the choice of different phonon scattering terms in our fitting procedure.

In the essential step of the analysis, we aimed at establishing the temperature dependence of the gap function $\Delta(T)$, using Eq. (7). The immediate result of this analysis is that a single gap function with the temperature dependence given by the BCS theory [20] is not adequate for MgB₂. The significant reduction of the low-temperature thermal conductivity by a rather weak magnetic field of 0.62 kOe (see Fig. 2) implies a strong interaction between phonons and the quasiparticles in the cores of the vortices induced by the magnetic field. In case of such a strong electron-phonon interaction and the formation of a single BSC-type gap, a significant change of the slope of $\kappa(T)$ at T_c is expected, as illustrated in Fig. 3, where the dotted line represents the calculation of $\kappa(T)$ for $\Delta(0) = 1.76k_B T_c$ and $\Delta(T)$ as tabulated in Ref. [20]. Hence, for the majority of quasiparticles involved in phonon scattering below T_c , the gap opens much more slowly with decreasing temperature than expected from the standard BCS prediction. Our fitting procedure is much more successful if we assume the formation of two energy gaps, as has previously

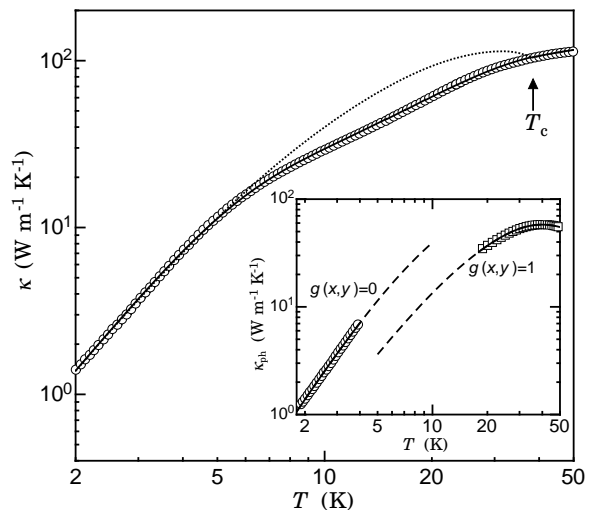


FIG. 3: In-plane thermal conductivity vs temperature in zero magnetic field. The solid line represents the best fit to the data assuming two gap functions (see text). The dotted curve results from a standard single-gap calculation with $\Delta(0) = 1.76k_B T_c$. The inset represents the phonon thermal conductivity κ_{ph} in the regime of negligible phonon-electron scattering ($H = 0$, open circles), and the open squares represent $\kappa_{\text{ph}}(T)$ at temperatures where the electron-phonon scattering is that of the normal-state ($H = 50$ kOe, $T \geq T_c$). The solid lines represent the fits described in the text.

been claimed in reports of other experimental studies of MgB₂. Thus, we consider two subsystems of quasiparticles with gaps Δ_1 and Δ_2 , different parameters E_1 and E_2 of phonon-electron scattering, and separate contributions κ_{e1} and κ_{e2} to the heat transport. The normal-state parameter E is then given by the sum $E = E_1 + E_2$. In the superconducting state, the last term in Eq. (7) adopts the form

$$E\omega [(1 - \alpha)g(x, y_1) + \alpha g(x, y_2)], \quad (8)$$

where $y_1 = \Delta_1(T)/k_B T$ and $y_2 = \Delta_2(T)/k_B T$. The parameter $\alpha = E_2/(E_1 + E_2)$ characterizes the relative weight of phonon scattering by quasiparticles in the two subsystems. Correspondingly,

$$\kappa_e = \frac{L_0 T}{\rho_0} [(1 - \delta)f(y_1) + \delta f(y_2)], \quad (9)$$

where the parameter $\delta = \kappa_{e2}/\kappa_e$ and $\kappa_e = \kappa_{e1} + \kappa_{e2}$. The fit is shown in Fig. 3 as the solid line.

The resulting values of the fit parameters are $\Delta_1(0) = 5.3 \pm 0.5$ meV, $\Delta_2(0) = 1.65 \pm 0.2$ meV, $\alpha = 1 \pm 0.02$ and $\delta = 0.33 \pm 0.02$. The ratio $2\Delta_1(0)/(k_B T_c) = 3.22$ is close to the weak-coupling BCS value of 3.52. The second gap, however, is considerably smaller. Our identification of two gaps is in qualitative and quantitative agreement with conclusions from results of specific heat,

point-contact spectroscopy, and photoemission experiments (see, e.g., Table I in Ref. [3]). The two gaps in MgB₂ are, by most authors, associated with different sheets of the Fermi-surface. According to density-functional calculations of Liu *et al.* [21], the smaller and the larger gap are associated with 3-dimensional sheets and 2-dimensional tubes, respectively. However, the first-principle FLAPW band calculations of Hase and Yamaji [22] claim the opposite. Our result of $\alpha = 1$ indicates that the dominant part of the interaction between quasiparticles and low-frequency phonons is provided by that part of the electronic excitation spectrum experiencing the smaller gap. The parameter E in Eq. (7) can be expressed as

$$E = \frac{m^* E_{\text{def}}^2}{2\pi v \hbar^3 D_0}, \quad (10)$$

where m^* is an effective electron mass, E_{def} is the deformation potential and D_0 is the mass density. The effective masses of quasiparticles on different parts of the Fermi surface of MgB₂ do not differ much [23]. It has been shown [24] that the interaction between the holes of the cylindrical σ -bands and the in-plane bond-stretching optical mode E_{2g} with a frequency of 470 cm⁻¹ is provided by an ultrastrong deformation potential. If E_{def} is also strong for low-frequency acoustic phonons of the same polarisation, then our result implies that it is the holes of the 2D sheets of the Fermi surface that experience the smaller energy gap, a counterintuitive result but in agreement with the conclusions of Ref. [22]. Considering the contributions of the two subgroups of quasiparticles to the heat transport, our result $\delta = 0.33$ suggests that the electrons experiencing the larger gap provide approximately 2/3 of total electronic heat conduction.

In conclusion, we present a study of the thermal conductivity κ in the ab -plane of a single crystal of MgB₂. The analysis of the temperature dependence of κ provides new convincing evidence for the formation of two superconducting gaps which are associated with different sheets of the Fermi surface.

Useful discussions with I. L. Landau, R. Monnier and F. Bouquet are acknowledged. This work was financially supported in part by the Schweizerische Nationalfonds zur Förderung der Wissenschaftlichen Forschung.

-
- [1] J. Nagamatsu, N. Nakagawa, T. Muranaka, Y. Zenitani, and J. Akimitsu, *Nature* **410**, 63 (2001).
 - [2] C. Busea and T. Yamashita, cond-mat/0108265 (unpublished).
 - [3] F. Bouquet *et al.*, cond-mat/0107196 (unpublished).
 - [4] J. Karpinski *et al.*, in preparation.
 - [5] N. Mott, *Proc. Phys. Soc.* **47**, 571 (1935).
 - [6] A. Wilson, *Proc. Roy. Soc.* **A167**, 580 (1938).
 - [7] M. Putti *et al.*, cond-mat/0109174 (unpublished).
 - [8] E. S. Clementyev, K. Conder, A. Furrer, and I. L. Sashin, *Eur. Phys. J. B* **21**, 465 (2001).
 - [9] T. Muranaka *et al.*, *J. Phys. Soc. Jpn.* **70**, 1480 (2001).
 - [10] S. L. Bud'ko *et al.*, *Phys. Rev. Lett.* **86**, 1877 (2001).
 - [11] C. Wälti *et al.*, *Phys. Rev. B* **64**, 172515 (2001).
 - [12] A. Junod, Y. Wang, F. Bouquet, and P. Toulemonde, cond-mat/0106394 (unpublished).
 - [13] M. Blackman, *Proc. Phys. Soc. A* **64**, 681 (1951).
 - [14] T. Muranaka, J. Akimitsu, and M. Sera, *Phys. Rev. B* **64**, 020505 (2001).
 - [15] E. Bauer *et al.*, *J. Phys.: Cond. Mat.* **13**, L487 (2001).
 - [16] M. Schneider *et al.*, *Physica C* **363**, 6 (2001).
 - [17] J. Bardeen, G. Rickayzen, and L. Tewordt, *Phys. Rev.* **113**, 982 (1959).
 - [18] R. Berman, *Thermal conduction in solids* (Clarendon Press, Oxford, 1976).
 - [19] S. Tsuda *et al.*, *Phys. Rev. Lett.* **87**, 177006 (2001).
 - [20] B. Mühlischlegel, *Z. Phys.* **155**, 313 (1959).
 - [21] A. Y. Liu, I. I. Mazin, and J. Kortus, *Phys. Rev. Lett.* **87**, 087005 (2001).
 - [22] I. Hase and K. Yamaji, *J. Phys. Soc. Jpn.* **70**, 2376 (2001).
 - [23] Y. Kong, O. V. Dolgov, O. Jepsen, and O. K. Andersen, cond-mat/0102499 (unpublished).
 - [24] J. M. An and W. E. Pickett, *Phys. Rev. Lett.* **86**, 4366 (2001).